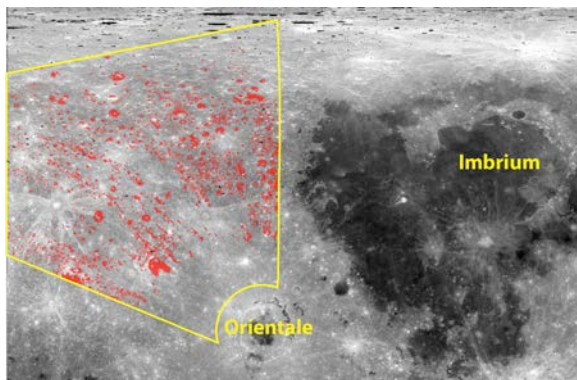


**LUNAR LIGHT PLAINS NEAR THE ORIENTALE AND IMBRIUM BASINS: RESULTS AND IMPLICATIONS FOR OTHER PLANETARY BODIES.** H. M. Meyer<sup>1,2</sup>, B. W. Denevi<sup>2</sup>, A. K. Boyd<sup>1</sup>, and M. S. Robinson<sup>1</sup>, <sup>1</sup>School of Earth and Space Exploration, Arizona State University, Tempe, AZ 85281 USA, <sup>2</sup>Johns Hopkins University Applied Physics Laboratory, Laurel, MD 20723 USA.

**Introduction:** Smooth plains deposits are typically the result of resurfacing from either impact ejecta or volcanism [e.g. 1,2]. On the Moon, most smooth plains within the highlands occur in crater floors and other topographic lows and are known as “light plains” due to their high albedo relative to the mare smooth plains (comparable to surrounding highlands) [3]. These light plains are generally thought to be of impact origin, though whether they are dominated by deposits from only the youngest large basins (i.e., Imbrium, Orientale) [4,5] or from a combination of many events [6] is not well known, and a volcanic origin for some regions has not been ruled out. Here we assess the origin of light plains by comparing their distributions with respect to the Orientale and Imbrium basins, their morphological relationships, and crater size–frequency distributions. Finally, we examine the implications of our lunar work for the origin of smooth plains deposits on other planetary bodies.

**Methods:** Light plains were mapped within a study area encompassing  $\sim 7.2$  million  $\text{km}^2$  (Fig. 1) using image mosaics with opposite solar azimuths from the LROC Wide Angle Camera (WAC) [7] at a pixel scale of 100 m. A map of the standard deviation of slope derived from the Global Lunar DTM (GLD 100) was used as an indication of roughness [8]. To determine the distribution of light plains with respect to the Imbrium basin, the study area (yellow in Fig. 1) was segmented into  $\sim 200$ -km bins at fixed radial distances from the basin rim. The area of light plains within each of the bins was normalized to the area of the bin (after subtracting out the area of large, superposed craters) to yield light plains areal percentage (Fig. 2). This process was then repeated for Orientale, dividing the



**Figure 1.** The light plains are mapped in red with the defined study area in yellow. The simple cylindrical projection is centered at  $260^\circ\text{E}$ . The basemap is WAC 643 normalized reflectance [9].

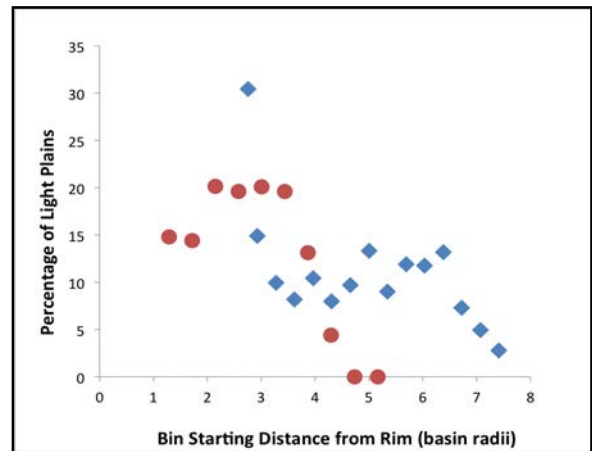


**Figure 2.** Percentage of light plains per bin with increasing distance from the rim of Imbrium (blue) and Orientale (red). Note that the first Imbrium bin, which is closest to the rim of Imbrium, shows the highest percentage of light plains. The Orientale bins dominated by the Hevelius formation have been removed to display only the distribution of the light plains.

same study area into  $\sim 200$ -km wide bins set at increasing radial distances from Orientale’s rim.

To assess age relationships among the light plains, 11 light plains areas were defined across our study area. For comparison, three areas were defined on the continuous ejecta of Orientale, which are used as a proxy for the age of the basin itself. Within each area, the crater size–frequency distribution was determined for craters greater than 1 km in diameter. Secondary craters were defined as irregularly shaped craters or those occurring in clusters or chains, and were excluded from these counts. Model ages were determined using the Neukum et al. [10] production function.

**Results:** Relative to Imbrium, the areal coverage of light plains is highest (30%) in the bin closest to Imbrium ( $\sim 2.8$  basin radii;  $\sim 1600$  km) and decreases to 15% in the second bin. After the first bin, the percentage of light plains is relatively stable at  $\sim 10\%$ , and then tapers off beyond the 12<sup>th</sup> bin. The distribution of light plains with respect to Orientale shows a different trend. There is relatively small fraction of plains in the fourth bin ( $\sim 1.3$ - $1.7$  basin radii). The highest percentage of light plains occur within bins 5-9 ( $\sim 1.7$ - $3.4$  basin radii from Orientale,  $\sim 800$ - $1800$  km), with  $\sim 15$ - $20\%$  light plains per bin area. Beyond  $\sim 1800$  km ( $\sim 3.9$  basin radii) from the rim there is a distinct dropoff in plains density to  $\sim 8\%$  in the tenth bin ( $\sim 3.9$ - $4.3$  basin radii) and  $\sim 5\%$  in the eleventh bin ( $\sim 4.3$ - $4.7$  basin radii).

Crater size-frequency distributions for the 11 areas within the study region yield age estimates ranging from 3.55 Ga to 3.88 Ga (Fig. 3). No clear spatial trend is observed among these ages, but the oldest ages are found in the eastern half of the study area. The areas within the continuous ejecta of Orientale yield model ages ranging from 3.67 Ga to 3.70 Ga. The count areas for our light plains deposits are relatively small, ranging from 5,000 – 25,000 km<sup>2</sup> with the total number of craters in each area ranging from 44 – 321. When the 11 light plains count areas are combined to account for limited areas and few craters, the age estimate is 3.73 Ga. There does appear to be some bias in the crater populations superposed on the light plains as there are no craters larger than 8 km within the light plains. This may be because craters greater than ~8 km sufficiently disrupt the unit to the point that it is no longer identifiable. When this discrepancy is accounted for by excluding of craters larger than 8 km from the continuous ejecta count areas, the age estimates for the continuous ejecta and the light plains are indistinguishable.

Distinct lobes and flow-like features link the light plains to the Hevelius Formation. In some areas, embayments are sharp with lobes overlying light plains, but in other areas flow-like features grade out from the Hevelius Formation into light plains deposits. In many regions light plains cluster around and appear to have flowed over Orientale secondary crater chains. No such morphological relationships to Imbrium are visible.

**Discussion:** The decreasing areal abundance of light plains with increasing distance from Orientale is consistent with emplacement during the Orientale impact event. Morphological relationships between the light plains and the Hevelius Formation, and the clustering of light plains along Orientale secondary crater chains, are also suggestive of a shared origin. Based on the distribution of light plains in our study area, a relationship between the light plains and the Imbrium basin is less clear, though the high abundance in the bin closest to the basin suggests material from the Imbrium event has contributed to the population of plains in the eastern portion of the mapping area. It is also possible that any preexisting light plains deposits from Imbrium were subsequently resurfaced by the deposits from the Orientale impact event. Crater size-frequency distributions show a slight increase in the ages of several count areas in the eastern side of the study area (Fig. 3); however, the combined statistics for the light plains produce an age estimate close to that of the continuous ejecta of Orientale. We interpret the majority of the light plains in our study area as being produced by the Orientale basin impact event, with material from the Imbrium event providing a secondary component.

*Implication for other planetary bodies:* Mercury's surface displays vast plains deposits, and their origin

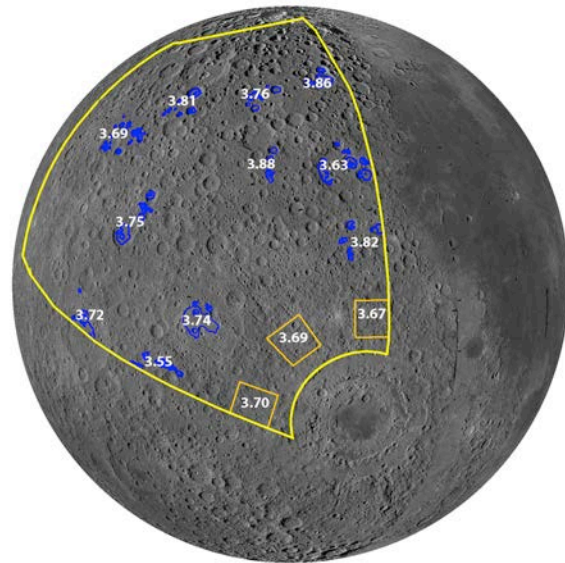


**Figure 3.** Count areas within the light plains and Orientale ejecta. Note that though the oldest areas are in the eastern portion of the study area, it also hosts some of the youngest model ages. Orthographic projection centered at 10°N, 250°E.

by either impact or volcanic resurfacing remains ambiguous [e.g., 2] and may be assessed by means similar to those in this work. Preliminary assessments of the distribution of intercrater plains around Beethoven basin (20°S 240°E, 643 km diameter), as mapped by Whitten et al. [11], suggest an origin distinct from that of the lunar light plains around Orientale [11]. The lunar light plains are patchy and discrete deposits, whereas the intercrater plains around Beethoven are larger and more consistent across the surface. The intercrater plains do not appear to cluster around secondary chains originating from Beethoven, as we observe for Orientale. There is no continuous ejecta deposit surrounding Beethoven equivalent to the Hevelius Formation around the Orientale basin. This could be due to differences in the cratering process on Mercury (e.g., larger component of impact melt within ejecta deposits) or to subsequent burial by volcanic deposits if such a continuous ejecta deposit existed. Further comparisons of the distribution, morphology, and ages lunar light plains with their Mercurian counterparts will provide insight into the formation processes of plains deposits of uncertain origin on Mercury.

**References:** [1] Young (1972) *NASA Apollo 16 Prelim. Sci. Rep.*, 5-1-5-6. [2] Denevi et al. (2013), *J. Geophys. Res. Planets*, 118, doi:10.1002/jgre.20075. [3] Wilhelms (1970) *Astrogeol. Stud. Ann. Prog. Report*, 13-28. [4] Eggleton and Schaber (1972) *NASA Apollo Prelim. Sci. Rep.*, 29-7-29-16. [5] Chao et al. (1975) *J. Res. U. S. Geol. Survey* 3, 379-392. [6] Oberbeck et al. (1974) *LPSC* 5, 111-136. [7] Robinson et al. (2010) *Space Sci. Rev.* 150, 81-124. [8] Scholten et al. (2011), *JGR*, 117, doi:10.1029/2011JE003926. [9] Boyd et al. (2013) *AGU Fall Meeting*, P13B-1744. [10] Neukum et al. (2001), *Space Sci. Rev.* 96, 55-86. [11] Whitten et al. (2014) *LPSC*, this conference.